SMA Technical Memorandum #54

Submillimeter Array

Antenna Mount Design Study

Abstract

This report summarizes the structural analysis for the Submillimeter Array antenna mount. The analysis considers wind and gravity loads and reports pointing errors and phase errors for these loading conditions. In general the performance goals for the mount have been achieved, and the mount performance is compatible with the overall budgets for antenna system performance.

Table of Contents

List of Figures

1. Description of Mount

The SMA antenna design concept currently consists of a modified nasmyth arrangement, with an equipment room which rotates in azimuth, but not elevation. The antennas are designed to be transported to fixed pads by a separate transport vehicle. Weight and stiffness are of critical design importance. Since the first two antennas will be assembled and tested off site, the design should be such to allow easy disassembly to parts of a manageable size for transportation.

The major design changes which have taken place since the Jan.'91 STAG Committee Meeting are:

a. Reduction of azimuth bearing diameter from 4 meters to 2.7 meters (and further reduction to 1.6 meters).

b. Reduction of elevation bearing spacing from 4 meters to 2.2 meters (and further reduction to 1.8 meters).

c. Relocation of the linear elevation drive attachment from the top of the reflector to the bottom (top and bottom with respect to reflector at horizon).

d. Changes to structural elements of mount to accommodate the above modifications.

The stationary race of the azimuth bearing is attached to a steel ring which is supported at 6 points on the foundation. Reducing the bearing diameter results in shorter spans between support points. This greatly increases the stiffness of the support ring and reduces the variation in gravity deflection as the antenna rotates in azimuth for a given number of support points.

Reduction of the elevation bearing spacing reduces the mount stiffness for wind-up about the azimuth axis due to applied torques. For an applied moment on the reflector, the resulting shear forces at the elevation bearings is inversely proportional to the bearing spacing. In addition, for a given pair of opposing tangential motions of the elevation bearings, the azimuth rotation of the reflector is also inversely proportional to the bearing spacing. In order to maintain azimuthal stiffness of the mount, it was necessary to increase the member sizes from 6"x6"x1/2" structural tubing to 12"x12"x1/2" and 12"x8"x1/2" tubing. The torsional stiffness of the mount remains less than the old design, and a means to measure the wind-up of the mount by using a shaft from the elevation axis down to the bottom of the mount will have to be included in the design.

Relocation of the linear elevation drive produces several effects. First, the drive screw has its lowest dynamic mode when the reflector is closest to the stationary end of the screw, acting as a cantilevered beam. By driving from the bottom of the reflector, this puts the cantilevered beam mode at the less critical low elevation viewing angles. Also, the elevation drive screw can now be supported by the cross-bracing elements in the center of the mount, without the need for a large additional supporting structure of the previous design. Another advantage of moving the drive to the bottom of the reflector is that the center of gravity of the drive rod (~165 kg.) does not move as much with elevation angle, reducing the mount deflection as the reflector moves in elevation.

Figure 1 illustrates the design concept for the mount as presented at the Jan. '91 STAG meeting, with the non-structural enclosures and equipment components removed for clarity. Figure 2 is the mount model with 2.7 meter azimuth bearing and relocated elevation drive, and Figure 3 is of the 1.6 meter azimuth bearing model.

Figure 1 - SMA Mount Design Concept at Jan. '91 STAG meeting

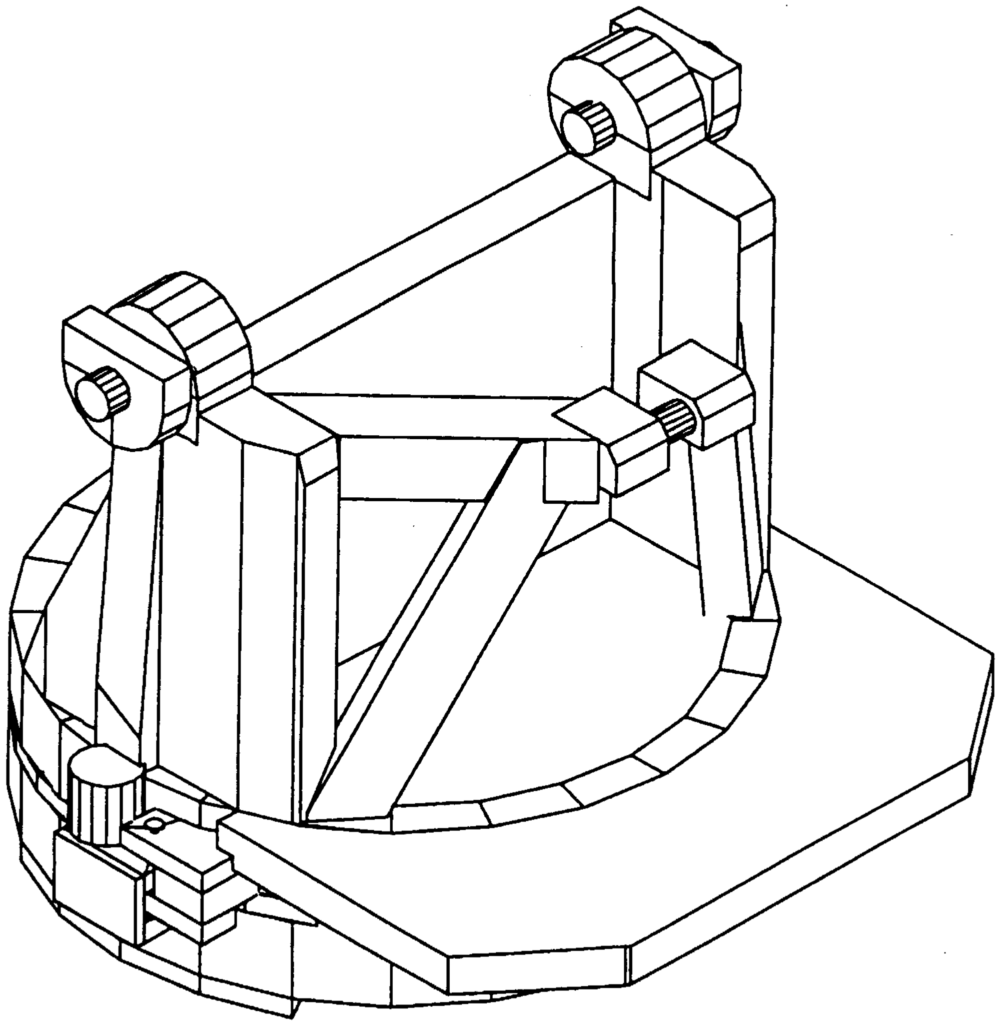

Figure 2 - SMA Mount Model with 2.7 meter azimuth bearing

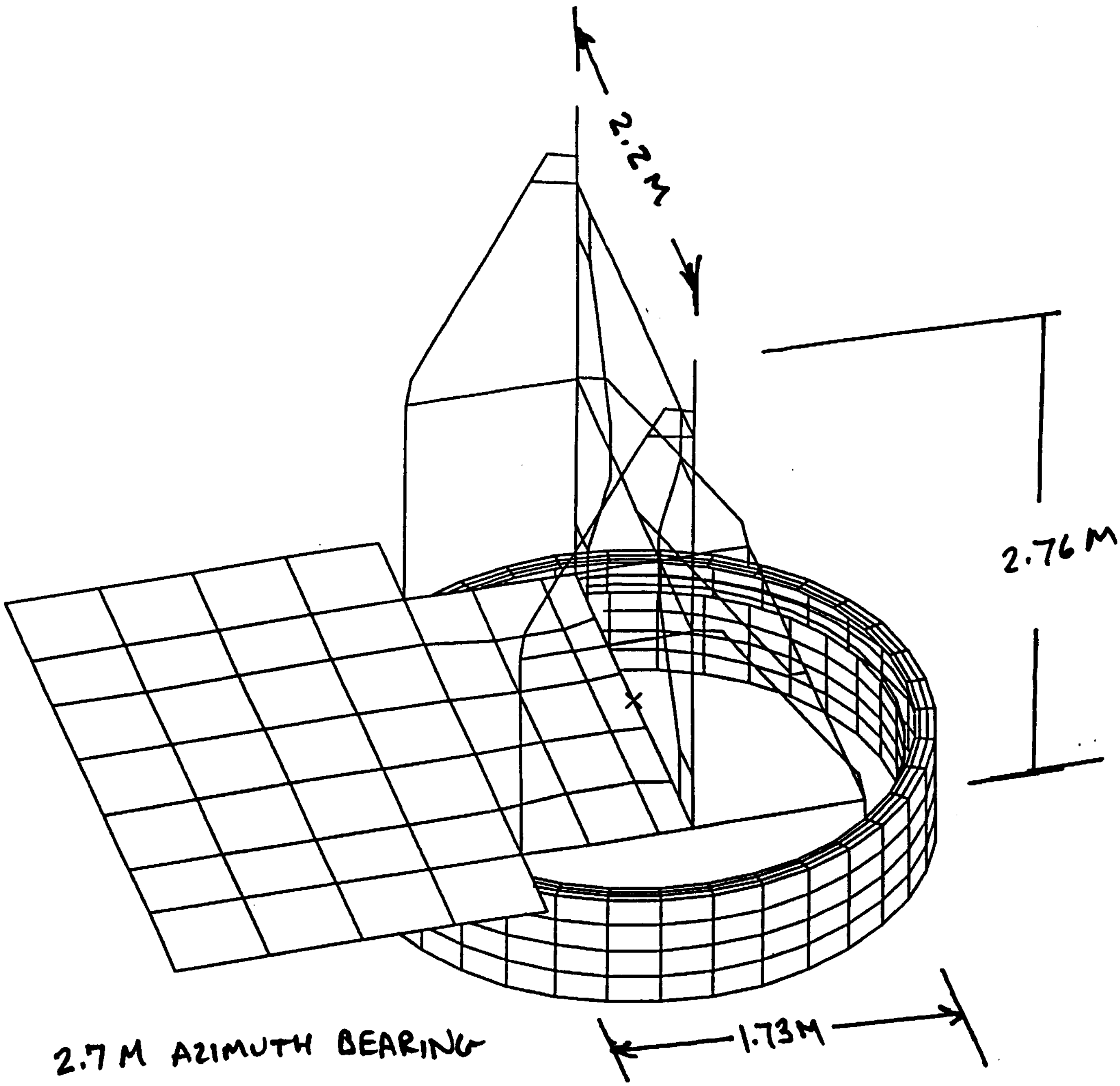

Figure 3 - SMA Mount Model with 1.6 meter azimuth bearing

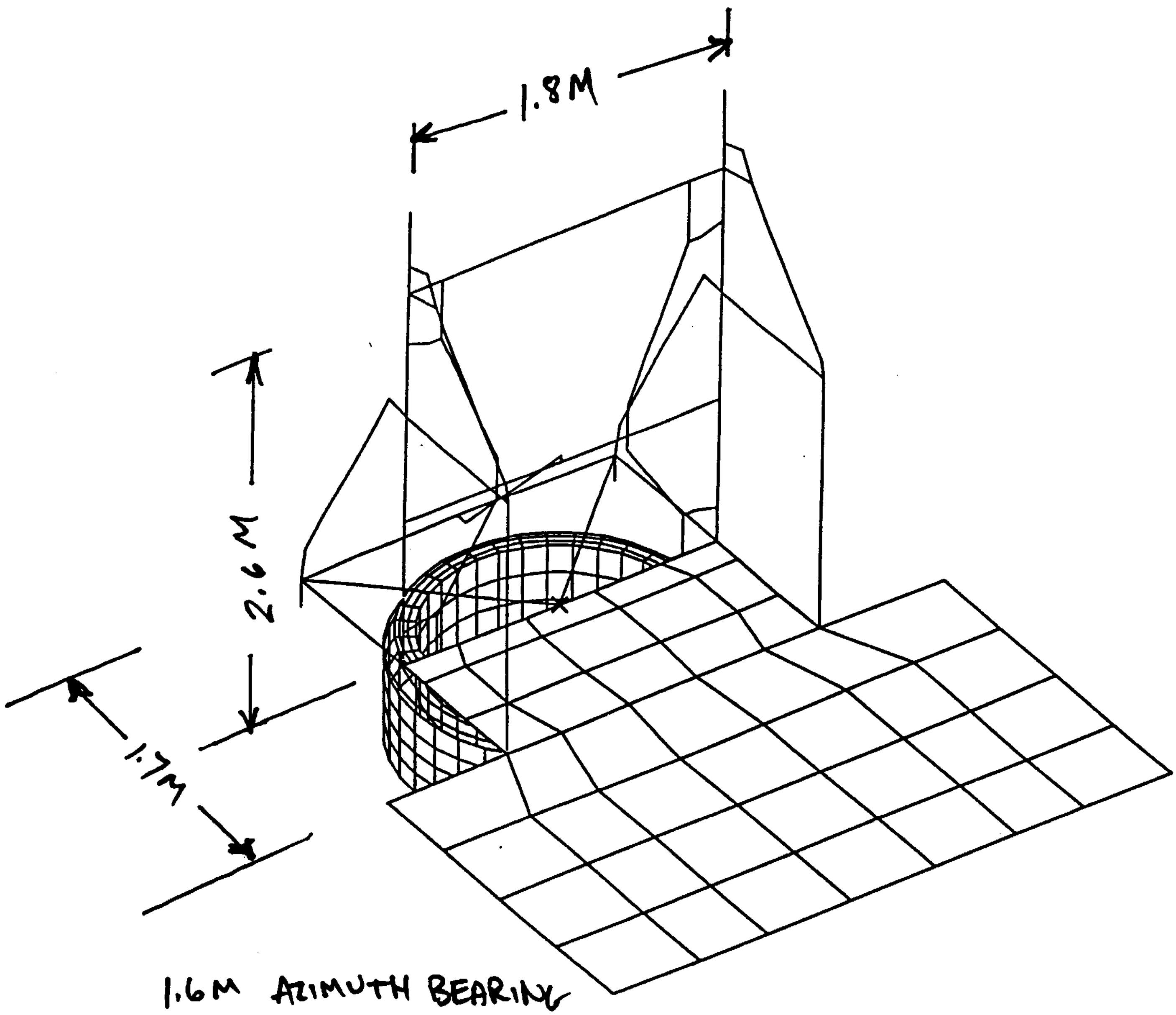

2. Design Requirements/Goals

The following parameters have been used as design requirements/goals:

1. Limit movement of the first fixed point at the intersection of the elevation and azimuth axes to less than 10 microns due to a 14 m/s wind load with an elevation angle at 45°.

2. Limit the peak rotation of the elevation encoder reference to less than 2.5 arc-sec for the peak gust component of a 14 m/s wind with an elevation angle of 45°.

3. Limit the peak variation between the elevation axis and the azimuth encoder sensed rotation to less than 0.3 arc-sec for the peak gust component of a 14 m/s wind with an elevation angle of 45°.

4. Limit variation in pointing as a function of azimuth angle for gravity loads to less than 0.2 arc-sec.

5. Limit variation in phase as a function of azimuth angle to less than 1 micron due to gravity.

6. Limit variation in elevation axis pointing as a function of elevation angle for gravity loads to less than 7.5 arc-sec for elevation angles of 30° to 90°.

7. Limit variation in phase as a function of elevation for gravity loads to less than 50 microns for elevation angles of 30° to 90°.

Frequencies	Natural frequencies of the antennas should be greater than 15 hz.
Transportability	Design should allow for pick-up points and means to position and secure to pad.
Weight	$<$ 22,500 kg

3. Finite Element Modeling

The finite element models used in this analysis have gone through several iterations during the design process. Variations in member cross sections, azimuth bearing size, frame layout, and support configurations have been evaluated in moving toward the current design.

The most recent design consists of a pair of nested azimuth bearing support rings, with the fixed outer ring attached to the bottom of the outer bearing race. The inner ring is attached to the top of the rotating race by a flange which also provides mounting locations for the rectangular framework of the upper mount. These support rings are modeled using 3"thk. plate elements.

The azimuth bearing races are modeled as 2 rings of beam elements with rigid beams from each node to the location of the rollers. Each pair of rigid beams around the circumference are connected by springs which represent the azimuth bearing stiffness, as discussed below.

The next layer of structure is a horizontal rectangular frame composed of 12"x12"x1/2" square structural tubing. This is attached to the flange of the outer bearing support ring at the 4 corners of the frame.

For the 2.7 m azimuth bearing model, above the rectangular frame is an A-frame type structure initially composed of 12"x12"x1/2" and 12"x8"x1/2" rectangular steel tubing. A second model was also used in which the upper frame structure was changed to 12" O.D. x 1" thk. round pipes.

Figure 4 shows the layout of the structure with rectangular tubes.

Figure 4 - 2.7 M Az. Bearing Mount Design

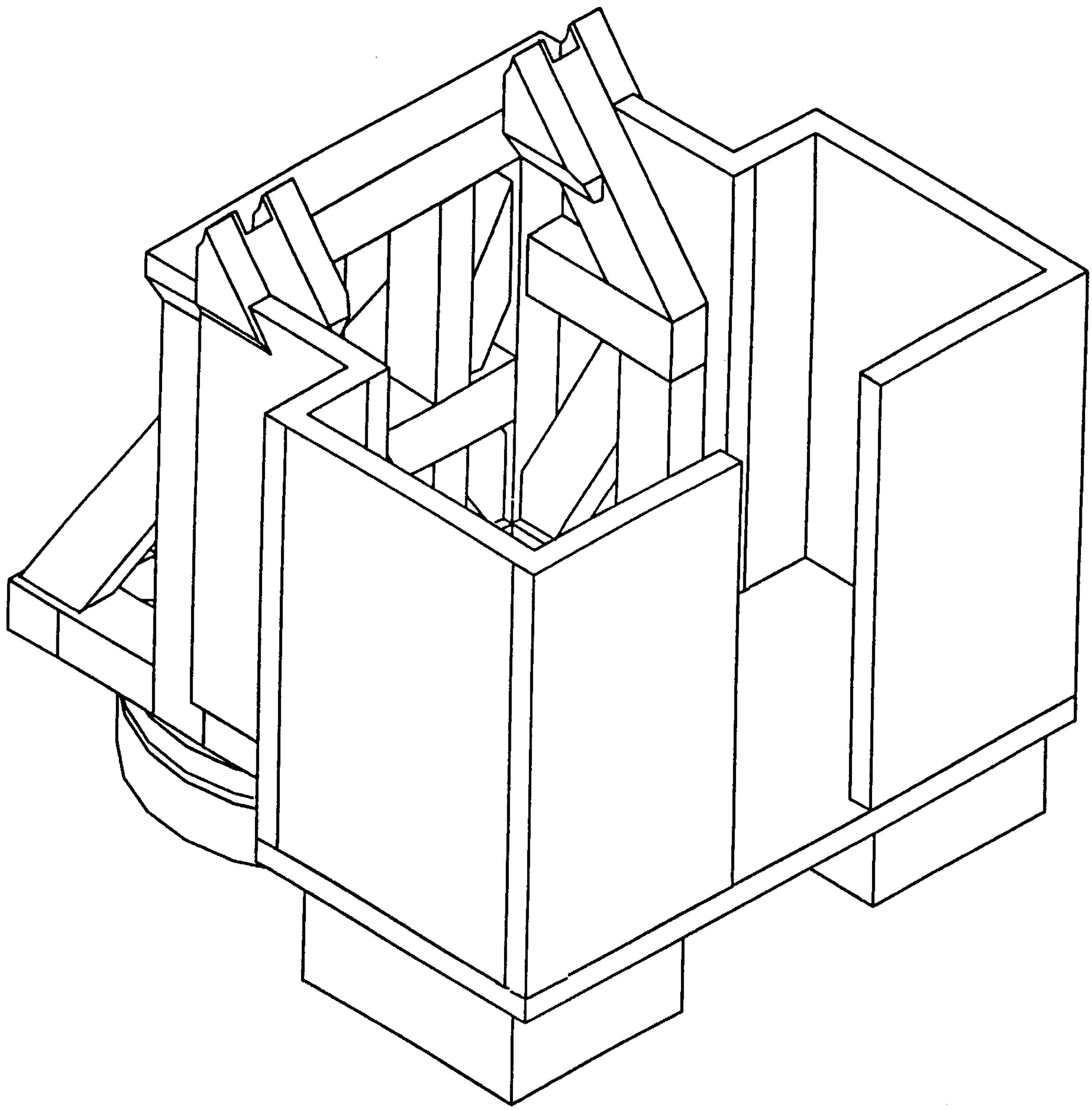

Mass Summaries

The following is a mass breakdown as modeled in I-DEAS for the 2.7 m azimuth bearing model:

Rotating ring & azimuth bearing race	4369 kg.
Fixed ring & azimuth bearing race	2606 kg.
Receiver cabin and equipment	4000 kg.
Elevation drive screw	165 kg.
Lower mount frame	1204 kg.
Upper Frame - option 1 (rectangular tubes)	2775 kg.
Upper Frame - option 2 (circular pipes)	4935 kg.
Total Mount Mass - Option 1	15120 kg.
Total Mount Mass - Option 2	17280 kg.

Total masses for all mount models are :

Az. Bearing Diameter	Elev. Bearing Spacing	Member Sizes	Mass
2.7 M	2.2 M	12"x12"x1/2" & 12"x 8"x1/2"	15120 kg.
2.7 M	2.2 M	12"x1" pipes	17280 kg.
1.6 M	1.8 M	12"x1" pipes	14000 kg.
1.6 M	1.8 M	16"x2" pipes	24280 kg.

Reflector Modeling

The bulk of the analyses were performed with the reflector modeled as a rigid element of various mass and inertias to represent several options of material and design of the panels and backstructure. In one set of runs, a full model of an intermediate reflector analysis was combined with the mount model to determine the effects of reflector flexibility on the dynamic response of the antenna.

Four cases of reflector masses were used during the course of these analyses. They represent various options of back-up structure and panel material choices.

Back-up structure	Panels	Mass	Model Designation
Carbon Fiber/Steel	Carbon Fiber	3153 kg.	(h7d33)
Carbon Fiber/Steel	Aluminum	5730 kg.	(bbdhal)
Carbon Fiber	Carbon Fiber	2070 kg.	(CF-CF)
Carbon Fiber	Aluminum	3070 kg.	(CF-AL)

Azimuth Bearing Modeling

The bearings being considered for azimuth rotation are Rotek Large Diameter Anti-Friction Bearings (Rotek Catalog #86). Stiffness information on a 90" cross-roller bearing has been obtained from Rotek. Examination of load vs. deflection curves from Kaydon Bearing catalog #300, indicates that the radial and axial stiffness vary linearly with diameter, for a size roller and spacing. It can be shown that the moment stiffness of these bearings is related to the axial stiffness by the equation:

K(Theta) = K(Axial)*(R**2)/2

Using this expression, the calculated moment stiffness of the 90" Rotek bearing is within 6% of the stiffness provided by Rotek. This indicates that a set of axial springs between the rotating and non-rotating bearing races will provide the correct axial and moment stiffness of the bearing.

The azimuth bearing is represented by a set of 36 spring elements spaced every 10 degrees around the circumference. Radial and axial stiffness are input, and this is sufficient to restrain the mount in all degrees of freedom except azimuthal rotation. The springs are assumed to act both in tension and compression, which reasonably represents the behavior of a preloaded bearing. The axial stiffness per spring is 1/36 of the total stiffness, while the radial stiffness per spring is 1/18 of the total stiffness, since all springs do not act in the same global direction.

The azimuthal rotation is restrained by two tangential springs between inner and outer races of the bearing. The stiffness of these springs was calculated to provide the rotational stiffness of the azimuth drive.

4. Analysis Load Cases

Gravity Loads

Gravity deflections were calculated for two elevation positions, zenith and 5° above horizon. This was accomplished by rotating the reflector node coordinates about the elevation axis to their new positions, then rotating the elevation drive screw about its pivot point to pick up the attachment point on the reflector, and tying the screw to the reflector with a pinned constraint at the appropriate point. Also, in order to assess the effect of having discrete support points on the fixed azimuth bearing ring, rather than a continuous support, six azimuthal positions were analyzed for both zenith and 5° by incrementing the six restrained nodes by 10° for each case.

Wind Loads - Precision Operation

Wind loading on the mount is a complex set of conditions which vary with wind speed and direction, and antenna position.

For wind loadings normal to the optical axis of the reflector, the reflector and backup structure is approximated by a cylinder 5.5 m diameter and 3.2 m long. Conservatively assuming sea level air density, a 14 m/sec wind produces a force of 2150 Newtons at a distance of 1.6 m from the elevation axis.

For wind directly into the reflector, a 6 meter diameter concave surface with a drag coefficient of 1.5 results in a force of 3717.8 Newtons on the reflector.

Three load cases are considered for wind normal to the optical axis and one case with wind straight into the reflector:

1. Reflector at horizon, wind parallel to elevation axis

2. Reflector at zenith, wind parallel to elevation axis

3. Reflector at zenith, wind perpendicular to elevation axis

4. Reflector at horizon, the wind directly into reflector.

Deformed geometry plots for the four wind cases are shown in Figures 7 through 10.

Frequency & Modeshapes

Frequencies and mode shapes were calculated at two reflector elevations, zenith and 5° above horizon. Most of the analyses were performed with rigid elements representing the mass and inertia of the reflector for 4 different material combinations. One case was run using an early reflector model, which resulted in a first mode frequency 30% less than the rigid model of the same mass. Although this model was not optimized for frequencies, it is reasonable to expect a 20% drop in frequency from the rigid cases. Not all combinations of reflector masses, mount design, and reflector elevation angles were run during the design/analysis iterations. The following is a summary of those cases which were run.

Reflector Model		------- 2.7 M Az. Bearing -----		
		Rectangular Members	Pipe Members	Pipe Members with 1.6 M Az. Bearing
h7d33 rigid	Zenith	16.0 hz	-	-
	5-deg.	-	-	-
h7d33 model	Zenith	11.5 hz	-	-
	5-deg.	-	-	-
bbdhal rigid	Zenith	10.4 hz	-	-
	5-deg.	-	-	-
CF-CF rigid	Zenith	18.4 hz	22.2 hz	-
	5-deg.	-	19.7 hz	-
CF-AL rigid	Zenith	15.3 hz	18.7 hz	13.3 hz-12" pipes
	5-deg.	-	17.6 hz	12.0 hz
				15.3 hz-16" pipes
				14.0 hz
CF-AL rigid 2 M Found.	Zenith	-	-	12.9 hz-16" pipes
	5-deg.	-	-	13.3 hz
CF-AL rigid 2.84 M Found	Zenith	-	-	14.6 hz-16" pipes
	5-deg.	-	-	13.7 hz

Mount Performance Evaluation

In order to assess the adequacy of the mount design for various load conditions, it is necessary to determine those factors which affect overall performance of the array. The reflector is attached to the mount kinematically to allow for relative thermal expansion without inducing strains in the reflector backstructure. Displacements of the 2 nodes representing the elevation bearings will induce phase and pointing errors in the antenna. Movement of the attachment point of the linear drive does not induce errors in pointing since that will be sensed by the elevation axis encoders.

Calculation of phase and pointing errors:

Early model runs did not have the lower bearing ring included, and the ring was considered rigidly mounted to a continuous foundation. For those analysis cases, the model gives no variation of deformation with azimuth position. Later runs investigate effects of 3 and 6 point mounting of the lower ring on mount performance.

The displacements (translations and rotations) of the two elevation bearing nodes are taken relative to the baseline case of 0 deg azimuth and 90 deg elevation (zenith). The displacements this baseline case are subtracted from each load case, and phase, elevation pointing and cross-elevation pointing errors are determined as follows (refer to Figure 5 for nomenclature and sign conventions):

dx of reflector is [dx(A)+dx(B)]/2

dy of reflector is [dy(A)+dy(B)]/2

dz of reflector not critical - always perpendicular to boresight

Th(x) of reflector is [dy(B)-dy(A)]/(distance from A-B)

Th(y) of reflector is [dx(A)-dx(B)]/(distance from A-B)

Th(z) of reflector is thz(A) and/or thz(B) since this rotates stationary side of elevation encoder(s).

Phase error depends on elevation angle (phi)

Phase = -dx*cos(phi)+dy*sin(phi)

Elevation pointing error is due to thz(A) and/or thz(B) rotating stationary side of encoder(s).

Cross elevation pointing error depends on elevation angle (phi)

X-EL = th(x)*sin(phi)+th(y)*cos(phi)

Figure 5 - Mount Performance Evaluation - Nomenclature and Sign Conventions

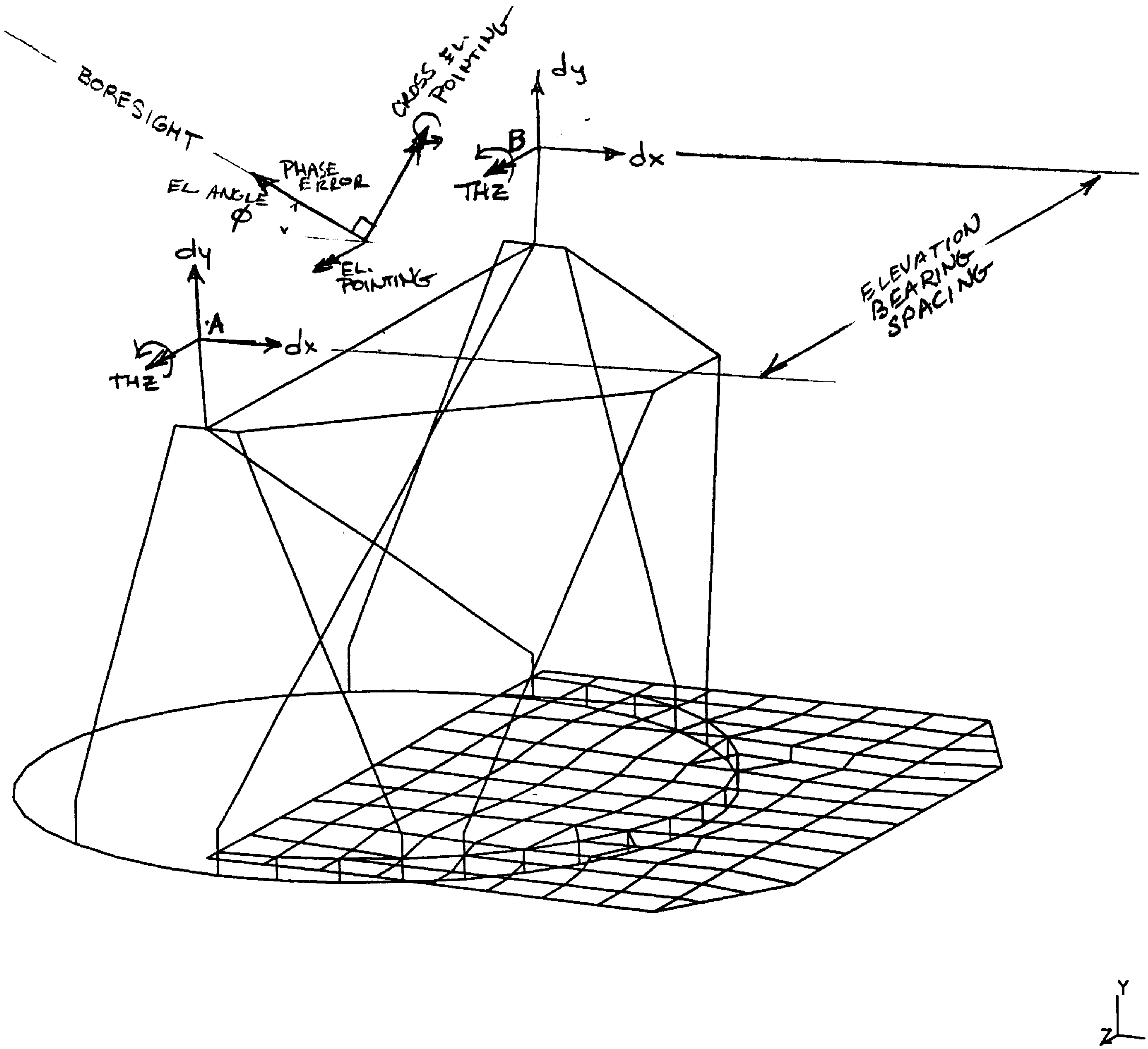

5. Soil/Foundation Analysis

The effects of soil stiffness and foundation geometry were determined with a solid model of the soil surrounding the foundation of the mount pad. The soil was modeled as a linear elastic material with a Young's modulus of 17660 psi, and a Poisson's ratio of 0.29, per Reference 1. The soil was modeled to a depth of 30 meters, and a diameter of 36 meters. A 180° cut-away view of the model is shown in Figure 6.

The foundation was represented as a rigid system for the purpose of this analysis. Two foundation configurations were analyzed. Both were truncated cones 1.56 meters thick. The first had an upper diameter of 2 meters, and a lower diameter of 3.76 meters. The second had an upper diameter of 2.84 meters, and a lower diameter of 4.6 meters. Unit deflections were applied to a node at the center of the top of the foundation, and the resulting stiffness matrices were used as input to the mount model.

The foundation stiffness was included in the latest mount model, 1.6 meter azimuth bearing, 16"x2" pipe members.

Foundation Stiffness:

Stiffness matrices are tabulated below for both the 2 meter and 2.84 meter diameter foundations. Units are newtons per meter and newton-meters per radian. The Y direction is vertical.

2 meter foundation

	X	Y	Z	RX	RY	RZ
X	1.172×10^9	0	0	0	0	1.655×10^9
Y	0	9.792×10^8	0	0	0	0
Z	0	0	1.172×10^9	-1.665×10^9	0	0
RX	0	0	-1.665×10^9	6.614×10^9	0	0
RY	0	0	0	0	7.061×10^9	0
RZ	1.655×10^9	0	0	0	0	6.614×10^9

2.84 meter foundation

	X	Y	Z	RX	RY	RZ
X	1.310×10^{9}	0	0	0	0	1.869×10^{9}
Y	0	1.102×10^{9}	0	0	0	0
Z	0	0	1.310×10^{9}	-1.869×10^{9}	0	0
RX	0	0	-1.869×10^{9}	8.933×10^{9}	0	0
RY	0	0	0	0	1.107×10^{10}	0
RZ	1.869×10^{9}	0	0	0	0	8.933×10^{9}

Figure 6 - Soil/Foundation Solid Element Model

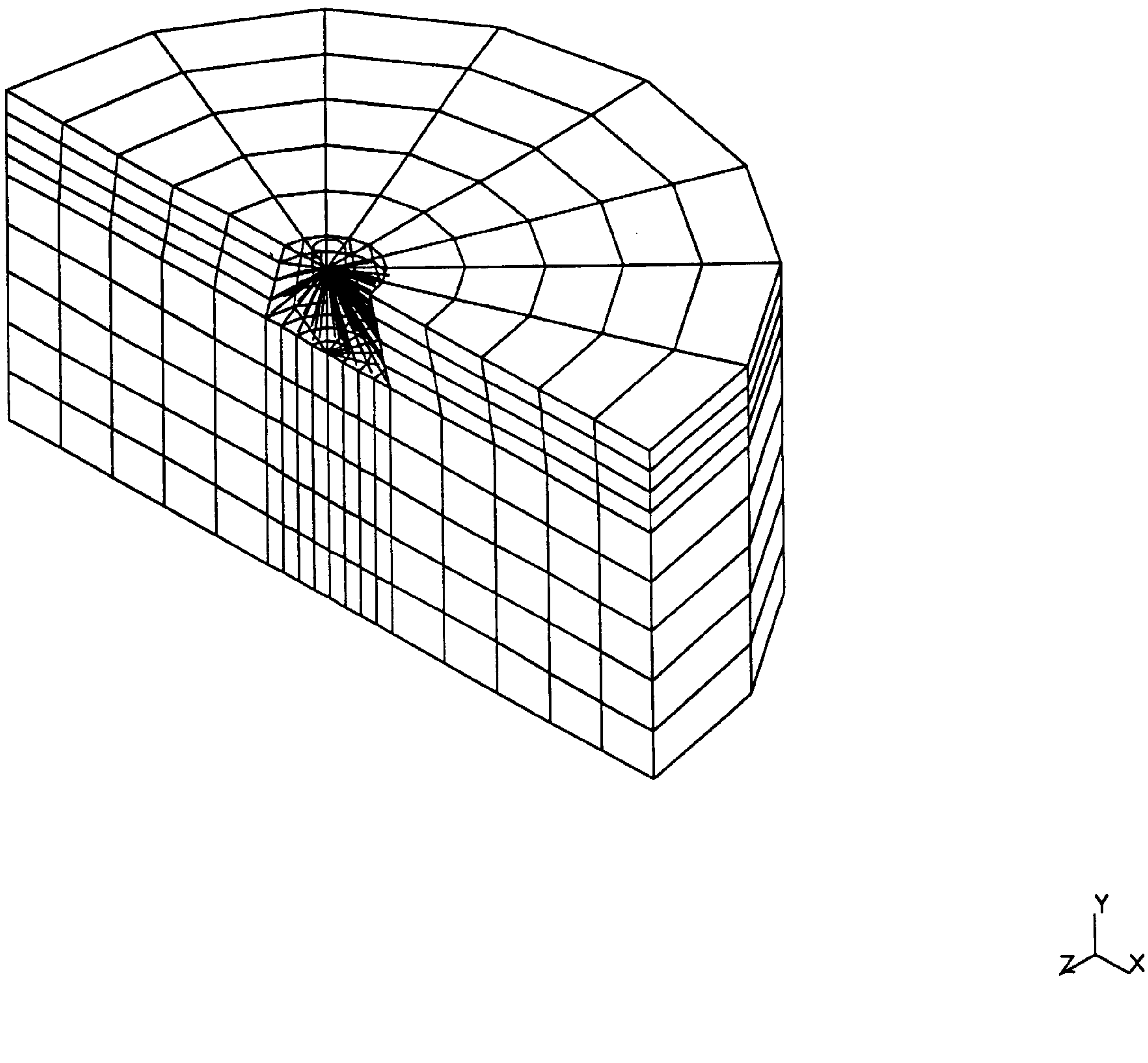

6. Analysis Summaries

Gravity Deflections

Summaries of gravity deflections are presented for the rectangular tube structure and for the round pipe structure for several reflector mass configurations.

Mount Configuration: Rectangular Tubing, 2.7 M Az. Bearing
Reflector : Dual Backstructure, Heavy Hub, Alum. Panels

Elevation Deg.	Azimuth Deg.	Phase Microns	Elevation pointing arc-sec		cross-el arc-sec
			Node A	Node B	
90.	0.	0.0000	0.0000	0.0000	0.0000
90.	10.	0.1700	0.0784	-0.0990	-0.0469
90.	20.	0.5200	0.0536	-0.1258	-0.0469
90.	30.	0.7100	-0.0474	-0.0474	0.0000
90.	40.	0.5200	-0.1258	0.0536	0.0469
90.	50.	0.1700	-0.0990	0.0784	0.0469
5.	0.	248.5872	50.3905	50.3905	0.0000
5.	10.	248.3513	50.4936	50.2667	-0.3464
5.	20.	247.8924	50.4317	50.2048	-0.3456
5.	30.	247.6608	50.2874	50.2874	0.0000
5.	40.	247.8924	50.2048	50.4317	0.3456
5.	50.	248.3513	50.2667	50.4936	0.3464

Mount Configuration: Rectangular Tubing, 2.7 M Az. Bearing
Reflector : CFRP Backstructure, Alum. Panels

Elevation Deg.	Azimuth Deg.	Phase Microns	Elevation pointing arc-sec		cross-el arc-sec
			Node A	Node B	
90.	0.	0.0000	0.0000	0.0000	0.0000
90.	10.	0.0850	0.0371	-0.0598	-0.0159
90.	20.	0.2750	0.0165	-0.0784	-0.0141
90.	30.	0.3800	-0.0413	-0.0413	0.0000
90.	40.	0.2750	-0.0784	0.0165	0.0141
90.	50.	0.0850	-0.0598	0.0371	0.0159
5.	0.	152.2649	31.8555	31.8555	0.0000
5.	10.	152.0792	31.9174	31.7524	-0.2632
5.	20.	151.7077	31.8968	31.7112	-0.2632
5.	30.	151.5238	31.7937	31.7937	0.0000
5.	40.	151.7077	31.7112	31.8968	0.2632
5.	50.	152.0792	31.7524	31.9174	0.2632

Mount Configuration: Rectangular Tubing, 2.7 M Az. Bearing
Reflector : CFRP Backstructure, CFRP Panels

Elevation Deg.	Azimuth Deg.	Phase Microns	Elevation pointing arc-sec Node A	Elevation pointing arc-sec Node B	cross-el arc-sec
90.	0.	0.0000	0.0000	0.0000	0.0000
90.	10.	0.0750	0.0330	-0.0516	-0.0159
90.	20.	0.2400	0.0165	-0.0681	-0.0150
90.	30.	0.3300	-0.0351	-0.0351	0.0000
90.	40.	0.2400	-0.0681	0.0165	0.0150
90.	50.	0.0750	-0.0516	0.0330	0.0159
5.	0.	99.6815	21.1607	21.1607	0.0000
5.	10.	99.4936	21.2020	21.0576	-0.2266
5.	20.	99.1182	21.1813	21.0369	-0.2265
5.	30.	98.9316	21.0988	21.0988	0.0000
5.	40.	99.1182	21.0369	21.1813	0.2265
5.	50.	99.4936	21.0576	21.2020	0.2266

Mount Configuration: 12" o.d. x 1" thk. Pipe 2.7 M Az. Bearing
Reflector : CFRP Backstructure, Alum. Panels

Elevation Deg.	Azimuth Deg.	Phase Microns	Elevation pointing arc-sec Node A	Elevation pointing arc-sec Node B	cross-el arc-sec
90.	0.	0.0000	0.0000	0.0000	0.0000
90.	10.	0.1300	0.0701	-0.0866	-0.0431
90.	20.	0.4200	0.0557	-0.1011	-0.0431
90.	30.	0.5800	-0.0309	-0.0309	0.0000
90.	40.	0.4200	-0.1011	0.0557	0.0431
90.	50.	0.1300	-0.0866	0.0701	0.0431
5.	0.	103.3161	23.1058	23.1058	0.0000
5.	10.	103.1250	23.1883	23.0027	-0.2582
5.	20.	102.7445	23.1470	22.9614	-0.2582
5.	30.	102.5451	23.0439	23.0439	0.0000
5.	40.	102.7445	22.9614	23.1470	0.2582
5.	50.	103.1250	23.0027	23.1883	0.2582

Mount Configuration: 12" o.d. x 1" thk. Pipe, 2.7 M Az. Bearing
Reflector : CFRP Backstructure, CFRP Panels

Elevation Deg.	Azimuth Deg.	Phase Microns	Elevation pointing arc-sec Node A	Node B	cross-el arc-sec
90.	0.	0.0000	0.0000	0.0000	0.0000
90.	10.	0.1250	0.0656	-0.0780	-0.0441
90.	20.	0.3900	0.0532	-0.0922	-0.0431
90.	30.	0.5300	-0.0262	-0.0262	0.0000
90.	40.	0.3900	-0.0922	0.0532	0.0431
90.	50.	0.1250	-0.0780	0.0656	0.0441
5.	0.	70.1474	15.6860	15.6860	0.0000
5.	10.	69.9703	15.7541	15.5911	-0.2282
5.	20.	69.6311	15.7293	15.5643	-0.2272
5.	30.	69.4698	15.6345	15.6345	0.0000
5.	40.	69.6311	15.5643	15.7293	0.2272
5.	50.	69.9703	15.5911	15.7541	0.2282

Mount Configuration: 12" o.d. x 1" thk. Pipe 1.6 M Az. Bearing
Reflector : CFRP Backstructure, Alum. Panels

Elevation Deg.	Azimuth Deg.	Phase Microns	Elevation pointing arc-sec Node A	Node B	cross-el arc-sec
90.	0.	0.0000	0.0000	0.0000	0.0000
90.	10.	-0.0050	-0.0041	-0.0041	-0.0057
90.	20.	-0.0050	-0.0103	-0.0103	-0.0057
90.	30.	0.0000	-0.0144	-0.0144	0.0000
90.	40.	-0.0050	-0.0103	-0.0103	0.0057
90.	50.	-0.0050	-0.0041	-0.0041	0.0057
5.	0.	198.0504	27.9159	27.9159	0.0000
5.	10.	198.0359	27.9138	27.9159	0.0718
5.	20.	198.0110	27.9118	27.9138	0.0684
5.	30.	198.0006	27.9118	27.9118	0.0000
5.	40.	198.0110	27.9138	27.9118	-0.0684
5.	50.	198.0359	27.9159	27.9138	-0.0718
30.	0.	142.9379	22.2704	22.2230	-0.0550

Mount Configuration: 16" o.d. x 2" thk. Pipe 1.6 M Az. Bearing
Reflector : CFRP Backstructure, Alum. Panels

Elevation Deg.	Azimuth Deg.	Phase Microns	Elevation pointing arc-sec Node A	Node B	cross-el arc-sec
90.	0.	0.0000	0.0000	0.0000	0.0000
90.	10.	-0.0050	-0.0021	0.0000	0.0011
90.	20.	-0.0100	-0.0021	0.0000	0.0000
90.	30.	-0.0100	-0.0021	-0.0021	0.0000
90.	40.	-0.0100	0.0000	-0.0021	0.0000
90.	50.	-0.0050	0.0000	-0.0021	-0.0011
5.	0.	71.5166	8.6796	8.6796	0.0000
5.	10.	71.5231	8.6796	8.6796	0.1547
5.	20.	71.5366	8.6796	8.6796	0.1520
5.	30.	71.5436	8.6796	8.6796	0.0000
5.	40.	71.5366	8.6796	8.6796	-0.1520
5.	50.	71.5231	8.6796	8.6796	-0.1547

Mount Configuration: 16" o.d. x 2" thk. Pipe 1.6 M Az. Bearing
Reflector : CFRP Backstructure, Alum. Panels, 2 M Foundation

Elevation Deg.	Azimuth Deg.	Phase Microns	Elevation pointing arc-sec Node A	Node B	cross-el arc-sec
90.	0.	0.0000	0.0000	0.0000	0.0000
90.	10.	0.0000	-0.0021	0.0000	0.0000
90.	20.	0.0000	-0.0021	0.0000	0.0000
90.	30.	0.0000	0.0000	0.0000	0.0000
90.	40.	0.0000	0.0000	-0.0021	0.0000
90.	50.	0.0000	0.0000	-0.0021	0.0000
5.	0.	124.3139	10.9795	10.9795	0.0000
5.	10.	124.3052	10.9774	10.9795	0.1553
5.	20.	124.3202	10.9774	10.9774	0.1518
5.	30.	124.3251	10.9774	10.9774	0.0000
5.	40.	124.3202	10.9774	10.9774	-0.1518
5.	50.	124.3052	10.9795	10.9774	-0.1553

Mount Configuration: 16" o.d. x 2" thk. Pipe 1.6 M Az. Bearing
Reflector : CFRP Backstructure, Alum. Panels 2.84 M Foundation

Elevation Deg.	Azimuth Deg.	Phase Microns	Elevation pointing arc-sec Node A	Node B	cross-el arc-sec
90.	0.	0.0000	0.0000	0.0000	0.0000
90.	10.	-0.0500	0.0000	0.0021	0.0115
90.	20.	-0.1000	0.0000	0.0000	0.0000
90.	30.	-0.1000	0.0000	0.0000	0.0000
90.	40.	-0.1000	0.0000	0.0000	0.0000
90.	50.	-0.0500	0.0021	0.0000	-0.0115
5.	0.	102.1249	10.2534	10.2534	0.0000
5.	10.	102.1314	10.2514	10.2534	0.1547
5.	20.	102.1449	10.2514	10.2534	0.1518
5.	30.	102.1528	10.2514	10.2514	0.0000
5.	40.	102.1449	10.2534	10.2514	-0.1518
5.	50.	102.1314	10.2534	10.2514	-0.1547

Wind Loads Deflection Summaries:

Phase and pointing errors for the wind cases are calculated like the gravity cases, except they are not taken relative to any other cases.

The phase and pointing errors of the mount for the analyzed wind cases are tabulated below:

Mount Configuration: Rectangular Tubing 2.7 M Az. Bearing

Elevation Deg.	Azimuth Deg.	Phase Microns	Elevation pointing arc-sec Node A	Node B	cross-el arc-sec	Wind Case
5.	90.	0.1696	-1.4144	1.4667	3.1536	1
90.	90.	-0.1115	0.6856	-0.6332	0.8499	2
90.	0.	1.9590	-3.1682	-3.1682	0.0000	3
5.	0.	-23.3233	-2.8465	-2.8465	0.0000	4

Mount Configuration: 12" o.d. x 1" thk. Pipe 2.7 M Az. Bearing

Elevation Deg.	Azimuth Deg.	Phase Microns	Elevation pointing arc-sec Node A	Node B	cross-el arc-sec	Wind Case
5.	90.	0.1227	-0.9952	1.0307	2.2127	1
90.	90.	-0.0775	0.5171	-0.4816	0.6506	2
90.	0.	1.3930	-2.2421	-2.2421	0.0000	3
5.	0.	-16.5759	-2.0257	-2.0257	0.0000	4

Mount Configuration: 12" o.d. x 1" thk. Pipe 1.6 M Az. Bearing

Elevation Deg.	Azimuth Deg.	Phase Microns	Elevation pointing arc-sec Node A	Node B	cross-el arc-sec	Wind Case
5.	90.	0.0700	-1.5080	1.5332	5.0832	1
90.	90.	-0.0545	0.4472	-0.4218	2.2628	2
90.	0.	0.3952	-3.6447	-3.6447	0.0000	3
5.	0.	-41.2592	-3.7375	-3.7375	0.0000	4

Mount Configuration: 16" o.d. x 2" thk. Pipe 1.6 M Az. Bearing

Elevation Deg.	Azimuth Deg.	Phase Microns	Elevation pointing arc-sec Node A	Node B	cross-el arc-sec	Wind Case
5.	90.	0.0278	-0.4325	0.4416	2.6458	1
90.	90.	-0.0240	0.0771	-0.0679	0.6866	2
90.	0.	0.0003	-1.1726	-1.1726	0.0000	3
5.	0.	-15.3838	-1.2308	-1.2308	0.0000	4

Mount Configuration: 16" o.d. x 2" thk. Pipe 1.6 M Az. Bearing
2 Meter Foundation

Elevation Deg.	Azimuth Deg.	Phase Microns	Elevation pointing arc-sec Node A	Node B	cross-el arc-sec	Wind Case
5.	90.	0.0278	-0.4325	0.4416	2.7882	
90.	90.	-0.0240	0.0771	-0.0679	1.3435	
90.	0.	0.0003	-1.8294	-1.8294	0.0000	
5.	0.	-38.6948	-2.1080	-2.1080	0.0000	

Mount Configuration: 16" o.d. x 2" thk. Pipe 1.6 M Az. Bearing
2.84 Meter Foundation

Elevation Deg.	Azimuth Deg.	Phase Microns	Elevation pointing arc-sec Node A	Node B	cross-el arc-sec	Wind Case
5.	90.	0.0328	-0.4325	0.4416	2.7344	
90.	90.	-0.0240	0.0771	-0.0679	1.0847	
90.	0.	0.0003	-1.5705	-1.5705	0.0000	
5.	0.	-28.1749	-1.7423	-1.7423	0.0000	

Deformed geometry plots for representative cases are shown in Figures 7 through 10.

Figure 7 - Mount Deformed Geometry - Wind Case 1

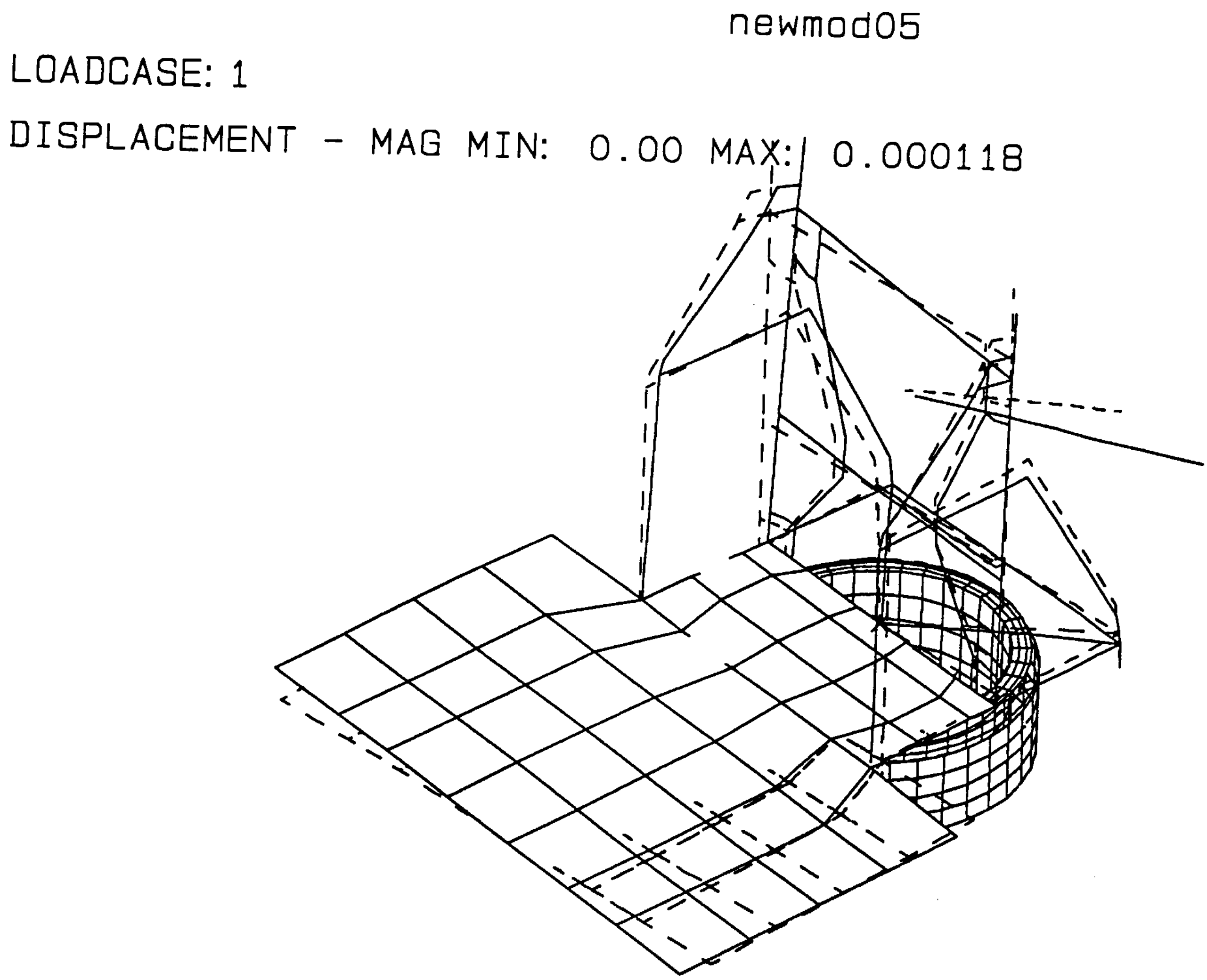

Figure 8 - Mount Deformed Geometry - Wind Case 2

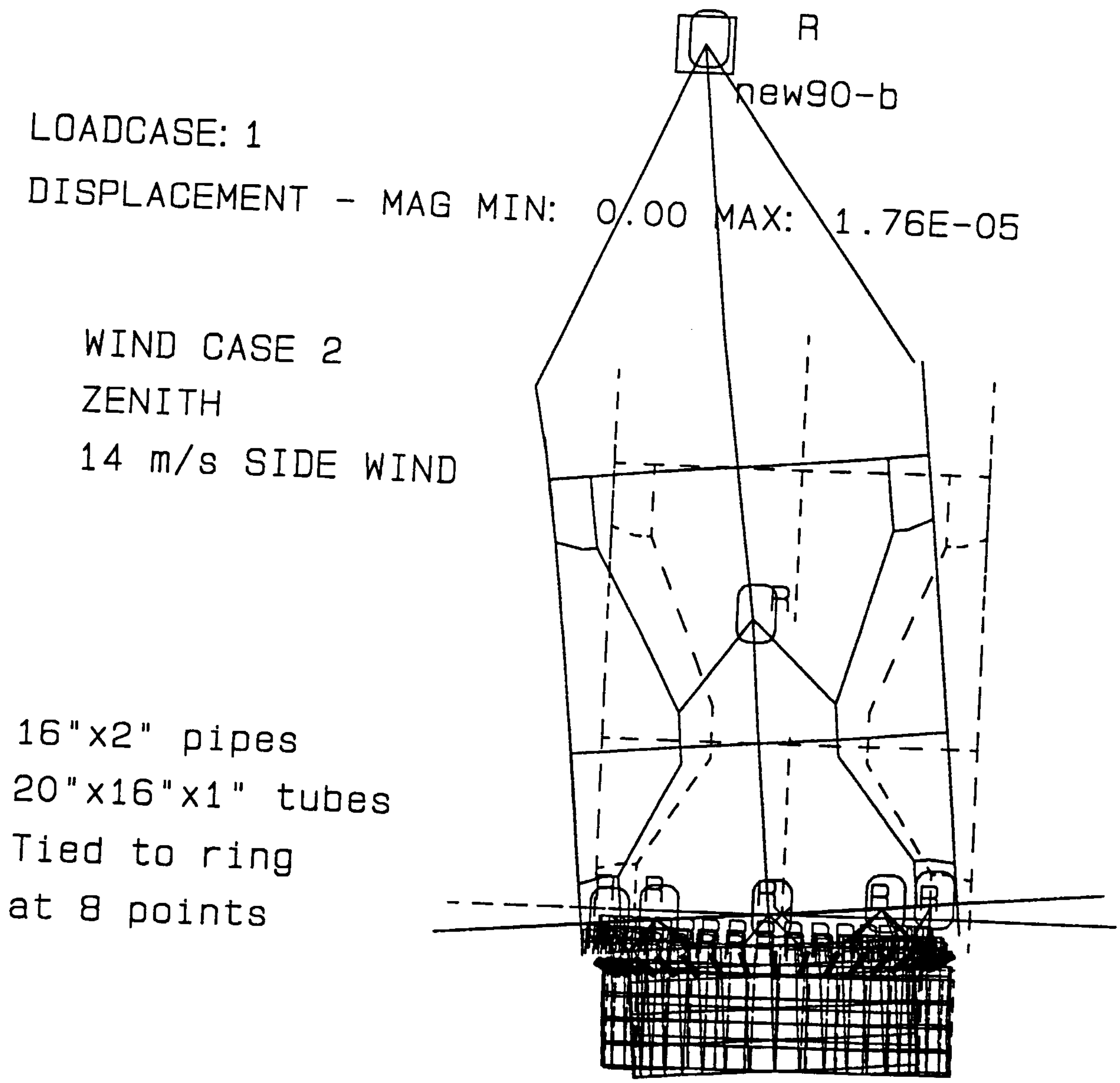

Figure 9 - Mount Deformed Geometry - Wind Case 3

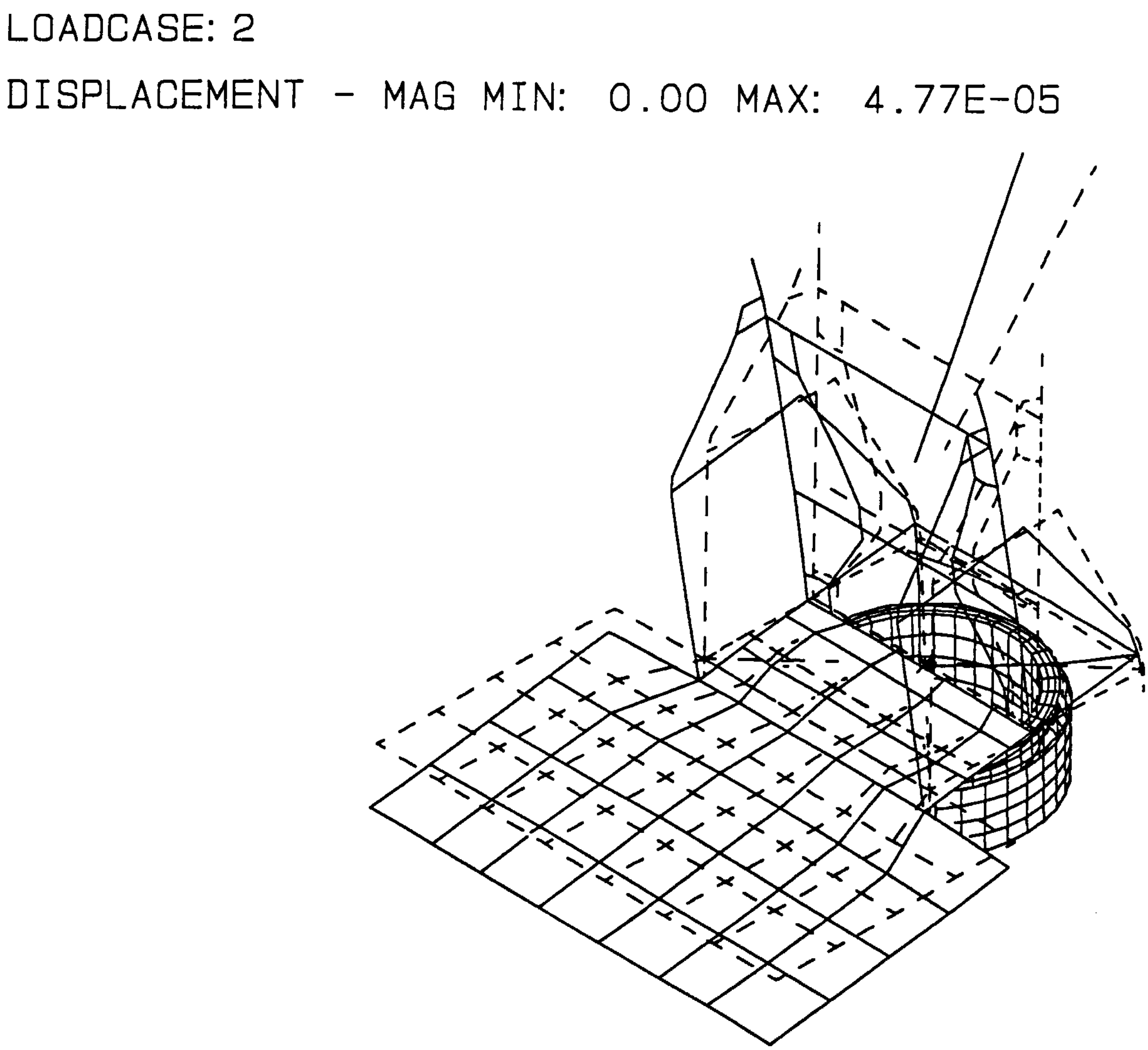

Figure 10 - Mount Deformed Geometry - Wind Case 4

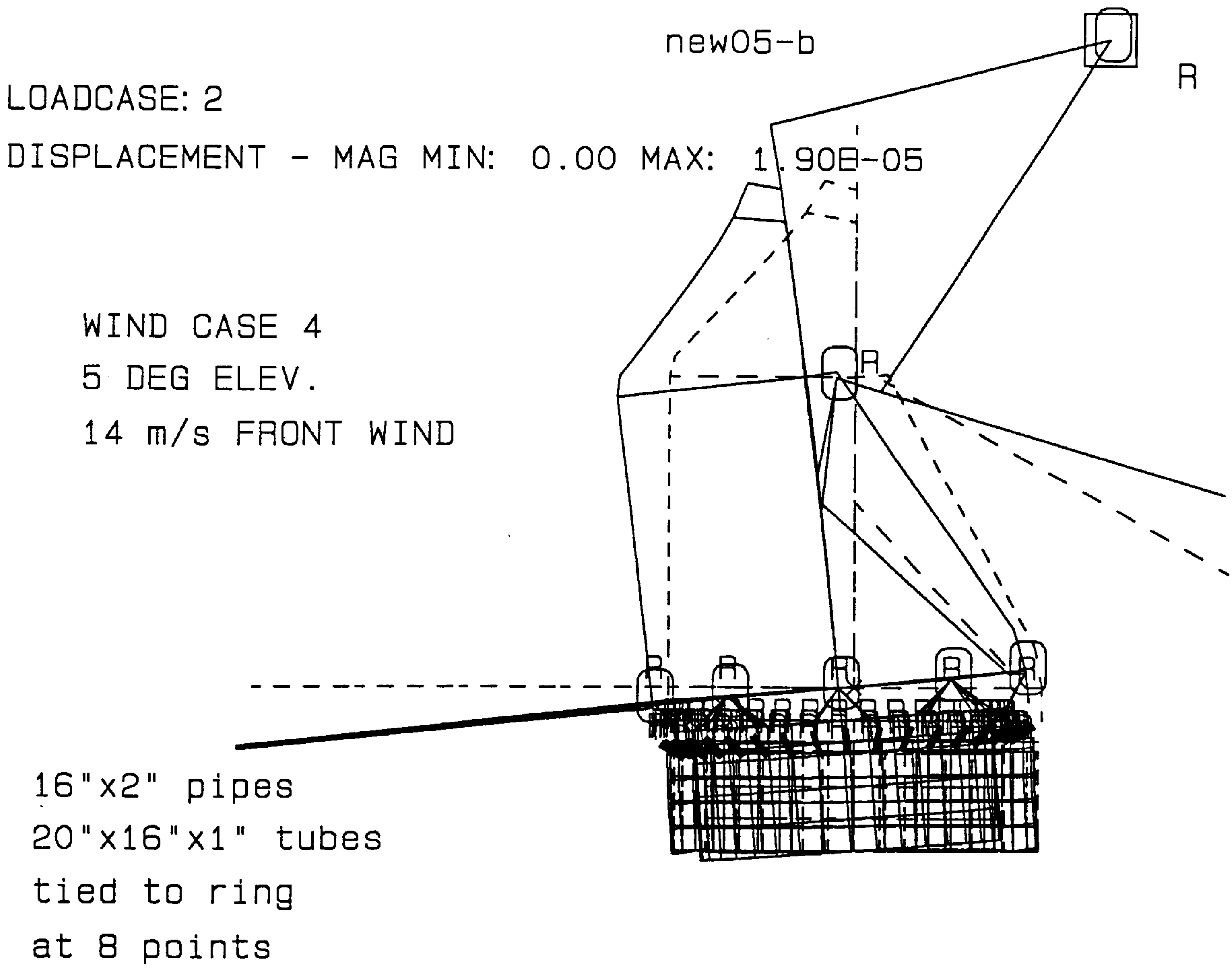

7. Conclusions

The predicted performance for the design with a 1.6 meter azimuth bearing and 16 inch O.D. round tubes with 2 inch wall thicknesses, versus the design goals/ requirements is summarized in the following table. The performance goals have not all been achieved. However, when the results are used in the overall budgets for the antenna system (see SMA Design Plan), the performance is acceptable. Futher work should be performed to optimize the structure for weight reduction and to determine the best mounting locations for the precision levels.

Performance Criteria	**Goal**	**Predicted Performance**
Movement of first fixed point (phase error) El. angle = 45 deg., 14 m/s wind gust	<10 microns	10.9 microns (15.4*cos(30))
Peak rotation of el. encoder reference for gust comp. of 14 m/s wind (Elevation Pointing Jitter)	<2.5 arc-sec.	1.3 arc-sec.
Peak variation of cross-el rotation of el axis relative to azimuth encoder sensed rotation (cross-el. pointing error)	<0.3 arc-sec.	0.4 arc-sec. (0.15*2.6)
Limit pointing variations as a function of azimuth angle for gravity loads	<0.2 arc-sec.	0.15 arc-sec.
Limit phase variations as a function of azimuth angle for gravity loads	<1 microns	0.02 microns
Limit pointing variations as a function of elevation angle for gravity loads	<7.5 arc-sec.	8.7 arc-sec.
Limit phase variation as a function of elevation angle for gravity loads	<50 microns	72 microns
Weight	<22,500 kg	24,280 kg
Resonant Frequency	>15 Hz	14 Hz

7. Conclusions

The predicted performance for the design with a 1.6 meter azimuth bearing and 16 inch O.D. round tubes with 2 inch wall thicknesses, versus the design goals/ requirements is summarized in the following table. The performance goals have not all been achieved. However, when the results are used in the overall budgets for the antenna system (see SMA Design Plan), the performance is acceptable. Futher work should be performed to optimize the structure for weight reduction and to determine the best mounting locations for the precision levels.

Performance Criteria	**Goal**	**Predicted Performance**
Movement of first fixed point (phase error) El. angle = 45 deg., 14 m/s wind gust	<10 microns	10.9 microns (15.4*cos(30))
Peak rotation of el. encoder reference for gust comp. of 14 m/s wind (Elevation Pointing Jitter)	<2.5 arc-sec.	1.3 arc-sec.
Peak variation of cross-el rotation of el axis relative to azimuth encoder sensed rotation (cross-el. pointing error)	<0.3 arc-sec.	0.4 arc-sec. (0.15*2.6)
Limit pointing variations as a function of azimuth angle for gravity loads	<0.2 arc-sec.	0.15 arc-sec.
Limit phase variations as a function of azimuth angle for gravity loads	<1 microns	0.02 microns
Limit pointing variations as a function of elevation angle for gravity loads	<7.5 arc-sec.	8.7 arc-sec.
Limit phase variation as a function of elevation angle for gravity loads	<50 microns	72 microns
Weight	<22,500 kg	24,280 kg
Resonant Frequency	>15 Hz	14 Hz

8. References

1. Soil Investigation, Keck Observatory 10-Meter Telescope, Mauna Kea, Hawaii, a report prepared for the University of California, Santa Cruz, Office of Campus Facilities, by Harding Lawson Associates, November 22, 1985.